The Journal of Nutrition
Biochemical, Molecular, and Genetic Mechanisms

Short-Chain Fatty Acids Activate AMP-Activated Protein Kinase and Ameliorate Ethanol-Induced Intestinal Barrier Dysfunction in Caco-2 Cell Monolayers[1,2]

Elhaseen E. Elamin,[3–5]* Ad A. Masclee,[3–5] Jan Dekker,[3,6] Harm-Jan Pieters,[4,5] and Daisy M. Jonkers[3–5]

[3]Top Institute Food and Nutrition, Wageningen, The Netherlands; [4]Department of Internal Medicine, Division of Gastroenterology–Hepatology, and [5]School for Nutrition, Toxicology, and Metabolism, Maastricht University Medical Center, Maastricht, The Netherlands; and [6]Department of Animal Sciences, Wageningen University, Wageningen, The Netherlands

Abstract

Short-chain fatty acids (SCFAs) have been shown to promote intestinal barrier function, but their protective effects against ethanol-induced intestinal injury and underlying mechanisms remain essentially unknown. The aim of the study was to analyze the influence of SCFAs on ethanol-induced barrier dysfunction and to examine the role of AMP-activated protein kinase (AMPK) as a possible mechanism using Caco-2 monolayers. The monolayers were treated apically with butyrate (2, 10, or 20 mmol/L), propionate (4, 20, or 40 mmol/L), or acetate (8, 40, or 80 mmol/L) for 1 h before ethanol (40 mmol/L) for 3 h. Barrier function was analyzed by measurement of transepithelial resistance and permeation of fluorescein isothiocyanate-labeled dextran. Distribution of the tight junction (TJ) proteins zona occludens-1, occludin, and filamentous-actin (F-actin) was examined by immunofluorescence. Metabolic stress was determined by measuring oxidative stress, mitochondrial function, and ATP using dichlorofluorescein diacetate, dimethylthiazol-2-yl-2,5-diphenyltetrazolium bromide, and bioluminescence assay, respectively. AMPK was knocked down by small interfering RNA (siRNA), and its activity was assessed by a cell-based ELISA. Exposure to ethanol significantly impaired barrier function compared with controls ($P < 0.0001$), disrupted TJ and F-actin cytoskeleton integrity, and induced metabolic stress. However, pretreatment with 2 mmol/L butyrate, 4 mmol/L propionate, and 8 mmol/L acetate significantly alleviated the ethanol-induced barrier dysfunction, TJ and F-actin disruption, and metabolic stress compared with ethanol-exposed monolayers ($P < 0.0001$). The promoting effects on barrier function were abolished by inhibiting AMPK using either compound C or siRNA. These observations indicate that SCFAs exhibit protective effects against ethanol-induced barrier disruption via AMPK activation, suggesting a potential for SCFAs as prophylactic and/or therapeutic factors against ethanol-induced gut leakiness. J. Nutr. 143: 1872–1881, 2013.

Introduction

Alcohol (or ethanol) is widely consumed and associated with development of chronic liver disease and gastrointestinal cancers (1). Experimental and clinical studies have demonstrated that ethanol is able to induce loss of tight junction (TJ)[7] integrity (2–4), leading to intestinal barrier dysfunction with subsequent translocation of luminal substances, such as bacterial endotoxins into the portal circulation and consequently liver injury (5–7). Ethanol-induced barrier dysfunction is considered to play a crucial role in the pathogenesis of alcoholic liver disease (ALD) (8,9) and can increase susceptibility to carcinogens (10). Because currently no effective therapy is available for ALD other than abstinence, restoring intestinal barrier integrity could be of distinctive value in preventing and/or treating ethanol-induced gut leakiness.

In the past decade, considerable research has been rekindled in prebiotics and their beneficial effects on intestinal health. SCFAs (<C8:0), including butyrate (C4:0), propionate (C3:0), and acetate (C2:0), are generated by bacterial fermentation of undigested carbohydrates, specifically resistant starches and dietary fiber, in the large intestine (11,12). Depending on diet and gut microbiota composition, intestinal concentrations can range from 60 mmol/L to 130 to 150 mmol/L (13), with butyrate,

[1] Supported by Top Institute Food and Nutrition.
[2] Author disclosures: E. E. Elamin, A. A. Masclee, J. Dekker, H.-J. Pieters, and D. M. Jonkers, no conflicts of interest.

[7] Abbreviations used: AICAR, aminoimidazole-4-carboxamide riboside; ALD, alcoholic liver disease; AMPK, AMP-activated protein kinase; Cc, compound C; DCF-DA, 2′,7′-dichlorodihydrofluorescein diacetate; F-actin, filamentous actin; FITC-D4, fluorescein isothiocyanate-labeled dextran 4 kDa; MTT, 3-(4.5-dimethylthiazol-2-yl)-2,5-diphenyltetrazolium bromide; pAMPK-α2, phosphorylated AMP-activated protein kinase-α2; ROS, reactive oxygen species; RT, room temperature; siRNA, small interfering RNA; TEER, transepithelial electrical resistance; TJ, tight junction; ZO-1, zona occludens-1.

* To whom correspondence should be addressed. E-mail: elhaseen.elamin@maastrichtuniversity.nl.

Manuscript received May 9, 2013. Initial review completed May 29, 2013. Revision accepted September 29, 2013.
First published online October 16, 2013; doi:10.3945/jn.113.179549.

propionate, and acetate in nearly constant molar ratios of 15:25:60, respectively (14). SCFAs have been demonstrated to exert many beneficial effects on intestinal epithelium, including inhibition of inflammation (15,16), modulation of oxidative stress (17), and prevention of colon carcinogenesis (18,19). Furthermore, an improved barrier function by SCFAs has been reported in vitro (20,21), ex vivo (22), and in animal studies (23). Mechanistic studies of the colon adenocarcinoma cell line Caco-2 have shown that butyrate enhances epithelial integrity by facilitating TJ assembly via increased activation of a number of cell signaling pathways, including AMP-activated protein kinase (AMPK) (24). AMPK plays a major role in cellular energy homeostasis and exerts cytoprotection under stressful conditions, such as hypoxia, ischemia, and oxidative stress (25).

Ethanol is a potent metabolic stressor and decreases cellular ATP production (26), which can be through modulation of AMPK, thereby contributing to increased intestinal permeability. However, the direct effects of the SCFAs, including butyrate, propionate, and acetate, on ethanol-induced barrier dysfunction and their possible mechanisms are essentially unknown. Therefore, we aimed to evaluate the potentially preventive effects of SCFAs on ethanol-induced TJ disruption in Caco-2 monolayers and to investigate involvement of metabolic stress and AMPK activation.

Materials and Methods

Cell line and culture conditions. Caco-2 cells (American Type Culture Collection; passage 39–48) were maintained in DMEM (Lonza Benelux) containing 4.5 g/L glucose and 0.29 g/L L-glutamine. The medium was supplemented with 10% (v:v) fetal calf serum (Invitrogen), 1% non-essential amino acids (Invitrogen), and 1% antibiotic/antimycotic mixture [10,000 U of penicillin, 10,000 μg of streptomycin, and 25 μg of amphotericin B per mL (Invitrogen)] at 37°C and in a 95% air/5% CO_2 atmosphere.

Transepithelial electrical resistance measurement. Caco-2 cells were grown for 21 d on collagen-coated permeable polycarbonate filters with a surface area of 0.33 cm^2 and 0.4 μm pore size (Costar). After developing transepithelial electrical resistance (TEER) > 600 $\Omega \cdot cm^2$, monolayers were exposed from the basal side to 40 mmol/L ethanol for 3 h in medium with or without luminal pretreatment with butyrate (2, 10, 20 mmol/L; Sigma-Aldrich), propionate (4, 20, 40 mmol/L; Sigma-Aldrich), or acetate (8, 40, 80 mmol/L; Sigma-Aldrich) solutions in medium with pH values ranging from 7.73 to 8.98 during incubation for 1 h. Because ethanol is volatile at 37°C, ethanol solutions were prepared at 4°C before the final working concentration and thereby counteracting evaporation. Next, Caco-2 monolayers were exposed in partly plastic tape-sealed plates, and ethanol in medium was replaced each hour to compensate for evaporation. In some experiments, monolayers were incubated with 0.01 mmol/L [6-(4-[2- pi peridin-1-yl-ethoxy]-phenyl)] 3-pyridin-4-yl-pyrazolo (1,5-a)pyrimidine (Sigma-Aldrich), a specific inhibitor of AMPK [known as compound C (Cc)] or 0.5 mmol/L 5-aminoimidazole-4-carboxamide riboside (AICAR; Sigma-Aldrich), an AMPK activator (27) for 1 h. TEER of epithelial monolayers (Ω) was measured after 60 or 180 min by an Epithelial Voltohmmeter (World Precision Instruments) in each insert and multiplied by the membrane surface area (0.33 cm^2), corrected by subtracting background resistance of the blank membrane (no cells; ~30 $\Omega \cdot cm^2$). Data were collected from duplicate inserts per treatment in 3 experiments and expressed as percentage of basal TEER obtained before treatment.

Determination of the paracellular permeability. Caco-2 cell monolayers were grown on Trans-well plates and treated as described above. By the end of TEER measurements, 1 g/L fluorescein isothiocyanate-labeled dextran 4 kDa (FITC-D4; Sigma-Aldrich) was added to the apical compartment and incubated for 1 h at 37°C. Then, 50 μL of medium from the apical and basal compartments were collected in 96-well plates, and FITC-D4 was measured spectrophotometrically at an excitation wavelength of 498 nm and an emission wavelength of 540 nm. Monolayer permeability was quantified as percentage of FITC-D4 permeating from the apical to the basal compartment.

Immunofluorescent analysis of zona occludens-1, occludin, and filamentous-actin localization. After incubation with ethanol with or without previous SCFA incubation, Caco-2 monolayers were fixed on the inserts for 10 min with 4% (wt:v) paraformaldehyde and permeabilized with 0.1% (v:v) Triton X-100 in PBS at room temperature (RT) for 40 min. Subsequently, mouse anti-zona occludens-1 (ZO-1; catalog #33-9100; Zymed Laboratories), rabbit anti-occludin (catalog #71-1500; Zymed Laboratories) (both 1:100 dilution in 3% wt:v BSA in PBS, pH 7.4), and Texas Red-X phalloidin (1:500 dilution in PBS, pH 7.4; catalog #T7471; Invitrogen) were used for immunofluorescent staining of ZO-1, occludin, and filamentous actin (F-actin), respectively, as described previously (3).

Determination of cellular F-actin contents. The relative content of F-actin was determined by a fluorescent phalloidin-binding assay as described previously (28). Briefly, Caco-2 cells grown on 96-well plates (Corning) were rinsed with PBS and then incubated with medium only, as well as ethanol (40 mmol/L) in medium for 3 h or after previous incubation with butyrate (2 mmol/L), propionate (4 mmol/L), or acetate (8 mmol/L) for 1 h. Next, the cells were fixed with acetone/methanol (1:1), and then actin was stained with rhodamine–phalloidin (1:500; catalog #R415; Invitrogen) diluted in PBS for 20 min. Stained cells were extracted with 200 μL of methanol and measured spectrophotometrically at excitation and emission wavelengths of 545 and 578 nm, respectively.

Detection of reactive oxygen species. Generation of H_2O_2 was monitored by using 2′,7′-dichlorodihydrofluorescein diacetate (DCF-DA; Sigma-Aldrich), which is nonfluorescent unless oxidized intracellularly by reactive oxygen species (ROS). Briefly, Caco-2 cells were cultured in 96-well plates and were loaded with 100 μM DCF-DA for 1 h at 37°C. Then, cells were exposed to 40 mmol/L ethanol for 3 h with or without previous treatment with 2 mmol/L butyrate, 4 mmol/L propionate, or 8 mmol/L acetate for 1 h. Medium-only and 40 mmol/L H_2O_2-treated cells were used as control conditions. Caco-2 cells were then washed twice in HBSS buffer, and the fluorescence was measured spectrophotometrically at excitation and emission wavelengths of 485 and 540 nm, respectively.

Assessment of mitochondrial function. Mitochondrial function was assessed using 3-(4.5-dimethylthiazol-2-yl)-2,5-diphenyltetrazolium bromide (MTT; Sigma-Aldrich) that is cleaved into insoluble formazan by active mitochondrial succinate dehydrogenases in living cells (29). Briefly, Caco-2 cells were cultured in 96-well plates and exposed to either 40 mmol/L ethanol in medium for 3 h or after previous treatment with 2 mmol/L butyrate, 4 mmol/L propionate, or 8 mmol/L acetate for 1 h. Medium only and 40 mmol/L H_2O_2 were used as negative and positive controls, respectively. The cells were washed with PBS and incubated with 5 g/L MTT in PBS, 200 μL/well for another 3 h at 37°C. Then, the solution was aspirated, and the insoluble formazan product was solubilized with 0.1 mol/L HCl in isopropanol (100 μL/well) and incubated at RT for 30 min. The optical density was measured at a wavelength of 560 nm. Values are presented as percentage of medium-only-treated cells.

Luminescent ATP assay. The amount of ATP produced by metabolically active cells was quantified based on the luciferase reaction (CellTiter-Glo Luminescent Cell Viability Assay; Promega). Briefly, Caco-2 cells were cultured in 96-well plates and exposed to 40 mmol/L ethanol in medium or after treatment for 3 h with 2 mmol/L butyrate, 4 mmol/L propionate, or 8 mmol/L acetate for 3 h. Then, plates were equilibrated at RT for 30 min. Thereafter, 100 μL of the assay reagent was added to each well. Medium only and 40 mmol/L H_2O_2 were used as negative and positive controls, respectively. Plates were placed on an orbital shaker for 2 min to induce cell lysis and then were incubated at RT for 10 min to stabilize the luminescent signal. The luminescence was measured spectrophotometrically. Intracellular

ATP was calculated from the luminescent values and presented as percentage of the medium-only-treated cells.

Assessment of AMPK activity. The activity of AMPK was assessed using a cell-based ELISA (RayBio cell-based protein phosphorylation ELISA kit; RayBiotech) according to the instructions of the manufacturer. Briefly, Caco-2 cells (20×10^3) were seeded in 96-well plates and incubated overnight at 37°C and 5% CO_2. Then, they were exposed to medium only as control and 40 mmol/L ethanol in medium for 3 h or after previous treatment with 2 mmol/L butyrate, 4 mmol/L propionate, or 8 mmol/L acetate for 1 h. Cells exposed to 0.01 mmol/L Cc (Sigma-Aldrich) and 0.5 mmol/L AICAR (Sigma-Aldrich) were used as negative and positive controls, respectively. After washing with PBS, 100 μL of fixative solution was added to each well and incubated for 20 min at RT with shaking. Then the plate was incubated with a quenching buffer for 20 min at RT. After that, a blocking solution was added, and the plate was incubated for 1 h at 37°C. Next, the plate was washed 3 times, and 50 μL of either rabbit anti-AMPK-α2 (catalog #2532L; Cell Signaling Technology) or rabbit anti-phosphorylated AMPK-α2 (pAMPK-α2; catalog #2535L, Cell Signaling Technology; Thr172, 1:100 dilution in the blocking solution, Cell Signaling Technology) was added and incubated for 1 h at RT with shaking. Next, 50 μL of HRP-conjugated mouse anti-rabbit IgG (1:100 dilution in the blocking solution; Dako Netherlands) was added and incubated for 1 h at RT. After washing 3 times, 100 μL of 3, 3′, 5, 5′-tetramethylbenzidine was added to each well and incubated for 30 min with shaking at RT in the dark. Finally, 50 μL stop solution ($2N\ H_2SO_4$) was added, and the optical density was read at an excitation wavelength of 450 nm.

Transfection of cells with AMPK small interfering RNA. Caco-2 (10^5 cells) at ~50% confluency were transfected with specific small interfering RNA (siRNA) targeting the mRNA encoding AMPK-α2 (Cell Signaling Technology) or control nonspecific siRNA (Santa Cruz Biotechnology), using Accell siRNA reagents (Dharmacon, Thermo Fisher Scientific), according to the protocol of the manufacturer. Briefly, 10^2 cells grown on either 96-well plates or 8-well chambers and 10^5 cells grown on transwell inserts (Costar) were incubated in serum- and antibiotic-free medium for 24 h. Then, cells were transfected with 50 nmol/mL of either AMPK-α2 siRNA or control nonspecific siRNA in Accell siRNA delivery medium (Dharmacon Thermo Fisher Scientific), gently shaken, and incubated at 37°C for 48 h and replaced thereafter with Accell delivery media. Cell-based ELISA assay with rabbit anti-AMPK-α2 (Cell Signaling Technology) was performed to monitor the efficiency of AMPK-α2 knockdown. In preliminary experiments, use of nonspecific siRNA resulted in no change in the cellular content of total AMPK-α2 or in the amount of pAMPK-α2 after AICAR exposure, and the transfection after 48 h was found to have 76% efficiency. The optimal concentration of siRNA was 50 pmol/mL because higher concentrations resulted in cell death. Finally, cells were treated with medium only, butyrate, propionate, and acetate, AICAR for 1 h, with or without ethanol exposure for another 3 h, followed by assessment of paracellular permeability.

Statistical analyses. Data are expressed as means ± SDs of triplicate experiments. One-factor ANOVA and when appropriate, Student's t test and 2-factor ANOVA were used for statistical analysis. Groups were compared by Tukey's post hoc test, considering a P value <0.05 as statistically significant. All data analyses were conducted with a GraphPad Prism software package (GraphPad Software).

Results

Effects of SCFAs on barrier function in Caco-2 cell monolayers. Caco-2 monolayers were treated with various concentrations of SCFAs to evaluate their effects on paracellular barrier function. Incubation with 2 mmol/L butyrate, 4 mmol/L propionate, or 8 mmol/L acetate led to a significant increase in TEER and a decrease in FITC-D4 permeation in Caco-2 monolayers (compared with controls, $P < 0.05$; **Fig. 1***A*, *B*). No significant differences were found for the other concentrations, apart from 80 mmol/L acetate, which significantly decreased TEER and increased FITC-D4 permeation ($P < 0.05$; Fig. 1*A*, *B*). The pH of each SCFA at the indicated concentrations measured by using a pH meter had no effect on Caco-2 monolayer permeability, apart from 80 mmol/L acetate (pH 8.47; data not shown). Subsequent experiments were performed using butyrate, propionate, and acetate at concentrations of 2, 4, and 8 mmol/L, respectively.

AMPK activation is involved in the regulation by SCFAs of the barrier function. To study the involvement of AMPK, we examined the phosphorylation status of AMPK-α2 after stimulation with SCFAs. As shown in **Figure 2***A*, the ratio of phosphorylated-to-total AMPK-α2 (pAMPK/total) increased significantly after treatment with butyrate, propionate, acetate, or AICAR (different from control, $P < 0.05$). Pretreatment with 0.01 mmol/L Cc significantly decreased pAMPK-α2/total ratios (different from treatment with butyrate, propionate, acetate, or AICAR, $P < 0.05$; Fig. 2*A*). Incubation with 2 mmol/L butyrate, 4 mmol/L propionate, or 8 mmol/L acetate, as well as with AICAR, also led to a significant increase in TEER (different from control, $P < 0.05$; Fig. 2*B*) and a significant decrease in FITC-D4 permeation (different from control, $P < 0.05$; Fig. 2*C*). These effects on TEER and FITC-D4 permeation were significantly abolished by pretreatment with Cc (different from treatment with butyrate, propionate, acetate, or AICAR, $P < 0.05$; Fig. 2*B*, *C*), respectively.

Effect of SCFAs on ethanol-induced changes in permeability. To establish whether SCFAs have potential to prevent ethanol-induced disruption of epithelial barrier function, the effects of butyrate, propionate, and acetate on the increase of intestinal epithelial TJ permeability induced by ethanol were investigated. Exposure to 40 mmol/L ethanol for 3 h significantly decreased TEER and increased FITC-D4 permeation of Caco-2

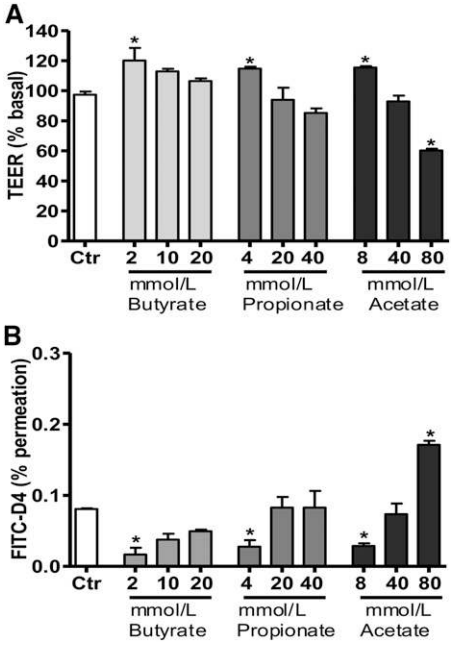

FIGURE 1 Effects of butyrate, propionate, and acetate on barrier function in Caco-2 cell monolayers. *A*, Percentage of basal TEER. *B*, Percentage of FITC-D4 permeation. Values are means ± SDs, $n = 9$. *Significantly different from Ctr, $P < 0.05$. Ctr, control; FITC-D4, fluorescein isothiocyanate-labeled dextran 4 kDa; TEER, transepithelial electrical resistance.

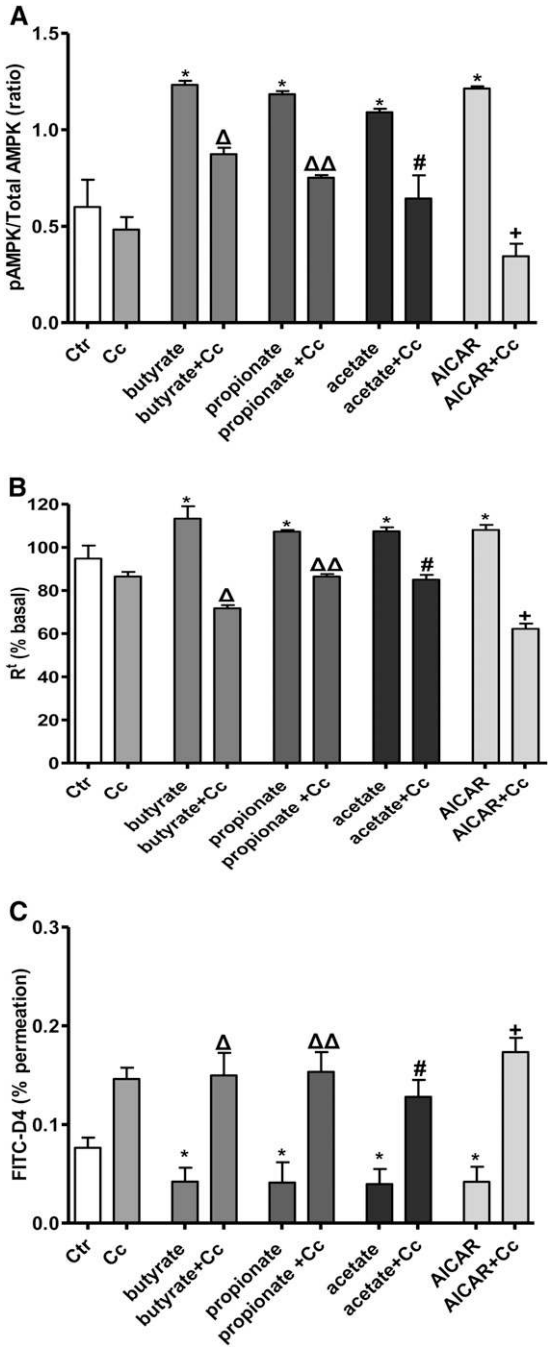

FIGURE 2 Effects of butyrate, propionate, acetate, and 5-AICAR (0.5 mmol/L) on AMPK activity and barrier function in Caco-2 cell monolayers with or without pretreatment with Cc (0.01 mmol/L). *A*, AMPK activity expressed as ratio of pAMPK-to-total protein (total AMPK). *B*, Percentage of TEER (R^t). *C*, Percentage of FITC-D4 permeation. Values are means ± SDs, $n = 3$. *Significantly different from Ctr, $P < 0.05$; $^{\Delta,\Delta\Delta,\#,+}$Significantly different from butyrate, propionate, acetate, and AICAR, respectively, $P < 0.05$. AICAR, aminoimidazole-4-carboxamide riboside; AMPK, AMP-activated protein kinase; Cc, compound C; Ctr, control; FITC-D4, fluorescein isothiocyanate-labeled dextran 4 kDa; pAMPK, phosphorylated AMP-activated protein kinase-α; TEER, transepithelial electrical resistance.

monolayers compared with medium-treated controls ($P < 0.05$; **Fig. 3***A*, *B*). Pretreatment with 2 mmol/L butyrate, 4 mmol/L propionate, or 8 mmol/L acetate for 1 h significantly prevented this drop in TEER and significantly decreased FITC-D4 permeation (different from treatment with ethanol, $P < 0.05$; Fig. 3*A*, *B*).

Effect of SCFAs on ethanol-induced changes in TJ proteins. In the absence of any treatment, microscopic analysis of immunofluorescently labeled ZO-1 and occludin showed that the distribution of ZO-1 was localized mainly in cell boundaries, was tightly arranged with sharp, continuous smooth edges, and showed a typical "chicken-wire" shape without abnormalities (Fig. 3*C*). Similarly, occludin was sharply localized around cell borders colocalizing with ZO-1 (Fig. 3*C*). Exposure to 40 mmol/L ethanol disrupted both ZO-1 and occludin networks and resulted in loss of colocalization and apparent gap formation between the cells (Fig. 3*C*, arrowheads). Pretreatment with butyrate, propionate, or acetate attenuated the changes induced by ethanol exposure (Fig. 3*C*).

Effects of SCFAs on ethanol-induced changes in F-actin organization and content. Because TJ disassembly can be induced by remodeling of perijunctional actin filaments, we next investigated whether the SCFAs can prevent changes in actin cytoskeleton junctions in ethanol-treated intestinal epithelial cells. Figure 3*D* shows that, under control conditions, apical F-actin microfilaments were assembled into a prominent perijunctional F-actin belt that encircled cell borders. Compared with controls, after ethanol exposure, the apical F-actin microfilaments were markedly disorganized, in which the perijunctional actin belt was transformed into an array of disordered filaments and stress fiber–like bundles (Fig. 3*D*, arrowheads). Such effects were attenuated by pretreatment with the SCFAs (Fig. 3*D*). In addition, exposure to ethanol as well as to the positive control H_2O_2 resulted in a significant increase in the intracellular F-actin content (different from control, $P < 0.05$; Fig. 3*E*). Pretreatment with SCFAs significantly reduced F-actin protein levels (different from treatment with ethanol, $P < 0.05$; Fig. 3*E*).

Effects of SCFAs on ethanol-induced cell metabolic stress. To evaluate the protective effects of SCFAs against ethanol-induced cellular metabolic stress, ROS production, mitochondrial function, and intracellular ATP levels were assessed. Exposure to 40 mmol/L ethanol or the positive control H_2O_2 significantly increased intracellular ROS generation and decreased mitochondrial function and ATP levels (different from negative controls, $P < 0.05$; **Fig. 4***A–C*). However, pretreatment of Caco-2 monolayers with 2 mmol/L butyrate, 4 mmol/L propionate, or 8 mmol/L acetate significantly prevented this ethanol-induced metabolic stress (different from treatment with ethanol, $P < 0.05$; Fig. 4*A–C*).

Effects of AMPK inhibition on SCFA-promoting effects on barrier function. To determine whether AMPK is involved in the promotion of barrier function by SCFAs in ethanol-treated monolayers, the effects of the SCFAs on ethanol-induced TEER decrease and FITC-D4 permeation in Caco-2 cell monolayers were compared with ethanol in medium, in the absence or presence of 0.01 mmol/L Cc. Incubation with 40 mmol/L ethanol for 3 h led to a significant decrease in TEER and an increase in FITC-D4 permeation (different from control, $P < 0.05$; **Fig. 5***A*, *B*, respectively). Pretreatment with 2 mmol/L butyrate, 4 mmol/L propionate, or 8 mmol/L acetate for 1 h significantly increased TEER values and decreased FITC-D4 permeation (different from ethanol, $P < 0.05$; Fig. 5*A*, *B*, respectively). These observations were significantly abolished by treatment with Cc (different from exposure to ethanol after pretreatment with SCFAs, $P < 0.05$; Fig. 5*A*, *B*, respectively). To complement the above observations, AMPK was knocked down by transfecting cells with specific siRNA targeting AMPK-α2. AMPK-α2 protein

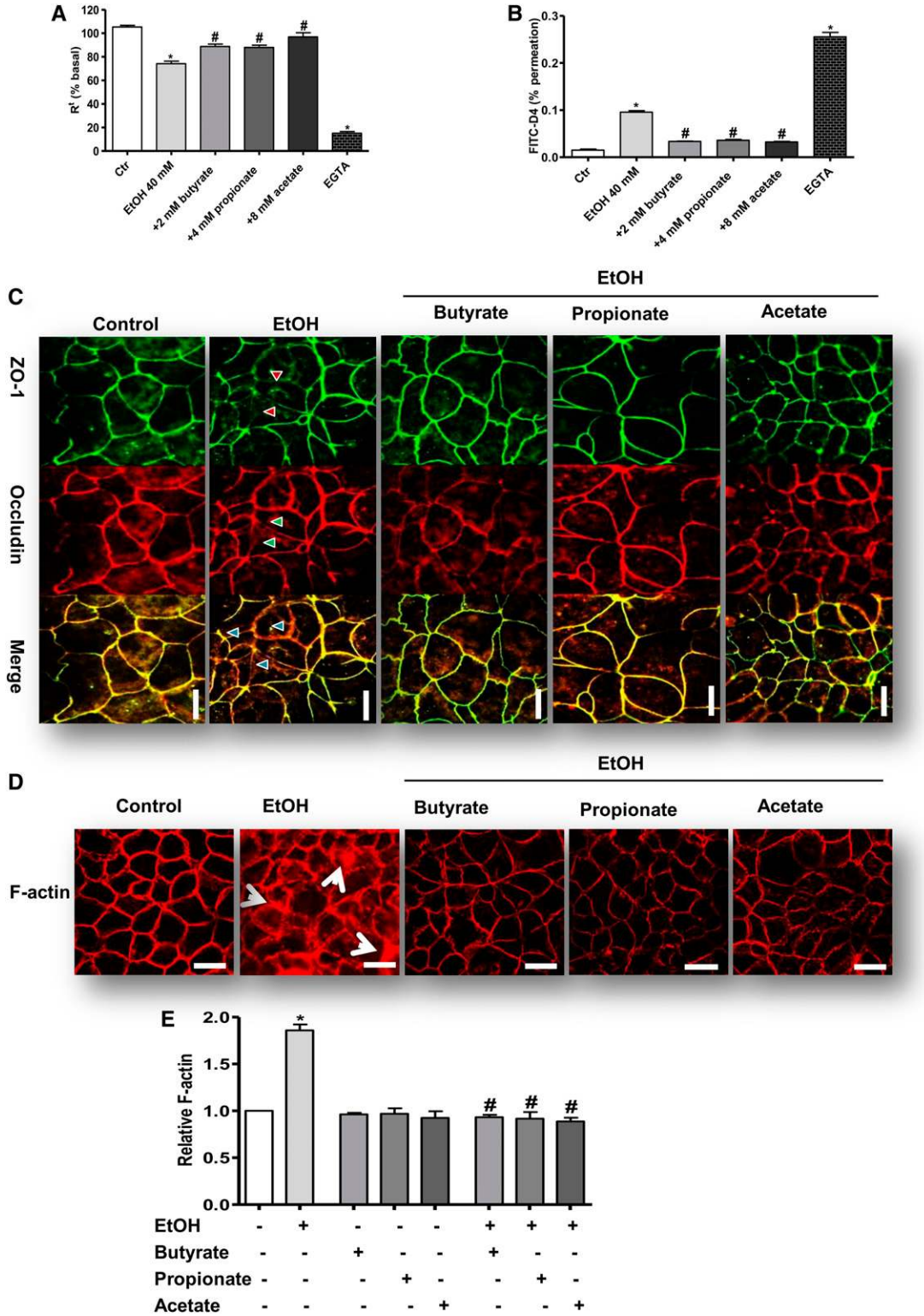

FIGURE 3 Effects of butyrate, propionate, and acetate on EtOH-induced loss of tight junction integrity in Caco-2 monolayers. EGTA was added as a control to destroy the tight junctions and to induce maximal reduction in TEER and FITC-D4 permeation. *A*, Percentage of basal TEER (R^t). *B*, Percentage of FITC-D4 permeation. Values are means ± SDs, $n = 9$. *Significantly different from Ctr, $P < 0.05$; #Significantly different from ethanol, $P < 0.05$. *C*, Representative images of immunostaining of ZO-1; (green) and occludin (red) as reproduced in 3 independent experiments, discontinuous staining and absence of ZO-1 and occludin colocalization, and gap formation are indicated by arrowheads in monolayers treated with ethanol. Scale bars, 10 μm. *D*, Distribution of F-actin in Caco-2 monolayers after staining with rhodamine–phalloidin dye (red) as reproduced in 3 independent experiments; condensation of F-actin and stress fiber–like bundles formation are indicated by arrowheads in monolayers treated with ethanol. Scale bars, 10 μm. *E*, F-actin contents in Caco-2 monolayers. Data bars represent the means ± SDs, $n = 3$. *Significantly different from Ctr, $P < 0.05$; #significantly different from ethanol, $P < 0.05$. Ctr, control; EGTA, ethylene glycol tetraacetic acid; EtOH, ethanol; F-actin, filamentous actin; FITC-D4, fluorescein isothiocyanate-labeled dextran 4 kDa; TEER, transepithelial electrical resistance; ZO-1, zona occludens-1.

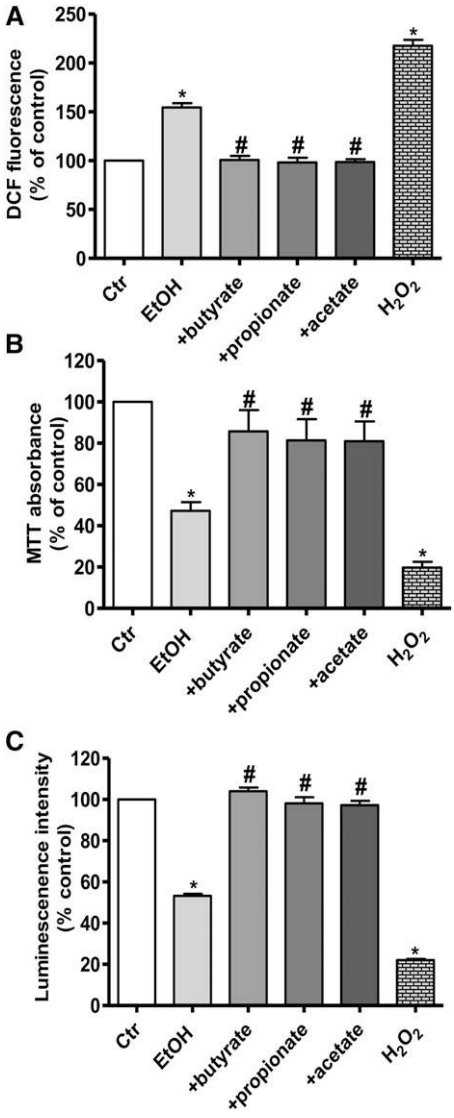

FIGURE 4 Effect of SCFAs on EtOH-induced cellular metabolic stress in Caco-2 monolayers incubated with butyrate, propionate, and acetate for 1 h, followed by ethanol for 3 h. *A*, Intracellular reactive oxygen species generation expressed as percentage of medium only-treated control. Mitochondrial function (*B*) and intracellular ATP levels (C). Values are presented as means ± SDs of 3 independent experiments. *Significantly different from Ctr, $P < 0.05$; #significantly different from 40 mmol/L ethanol, $P < 0.05$. Ctr, control; DCF, 2′,7′-dichlorodihydrofluorescein diacetate; EtOH, ethanol; MTT, 3-(4.5-dimethylthiazol-2-yl)-2,5-diphenyltetrazolium bromide.

level was significantly reduced (76%) by specific siRNA transfection ($P < 0.01$; **Fig. 6***A*). Compared with monolayers transfected with nonspecific siRNA, knockdown of AMPK-α2 with specific siRNA significantly abolished the ability of butyrate, propionate, and acetate (all $P < 0.01$) to mitigate the ethanol-induced TEER decrease (Fig. 6*B–D*, respectively). Furthermore, siRNA specific for AMPK-α2, but not control siRNA, also significantly dampened the ability of butyrate, propionate, and acetate (all $P < 0.01$) to alleviate the ethanol-induced FITC-D4 permeation (Fig. 6*E–G*, respectively).

Discussion

The present study demonstrates that butyrate, propionate, and acetate attenuate ethanol-induced intestinal epithelial TJ barrier dysfunction in Caco-2 monolayers. SCFAs did also partially prevent the displacement of TJ proteins and stress-fiber formation as well as the ethanol-induced cellular oxidative and metabolic stress. We found that this beneficial effect of SCFAs was mediated by the activation of the AMPK pathway.

In the current study, we found that incubation of intestinal Caco-2 cells with 40 mmol/L ethanol increased monolayer permeability, altered morphologic appearance of the TJ, and increased F-actin protein expression. The concentration of ethanol used in our study is not cytotoxic as shown previously that ethanol at a concentration of 0.2% v:v (~40 mmol/L), which can be achieved in blood after moderate (2–4 drinks; 1 standard drink, ~14 g of ethanol) consumption (30,31), can disrupt epithelial TJ integrity in a Caco-2 3-dimensional cell culture model without compromising cell viability (3). Our findings are also in agreement with previous observations by others showing that ethanol can disrupt the TJ integrity, resulting in increased paracellular permeability (30,32–34).

Cellular metabolic stress, including increase in oxidative stress and decrease in ATP production, is suggested to be involved in loss of TJ integrity (35). Here, we present evidence that ethanol not only disrupts paracellular permeability but also

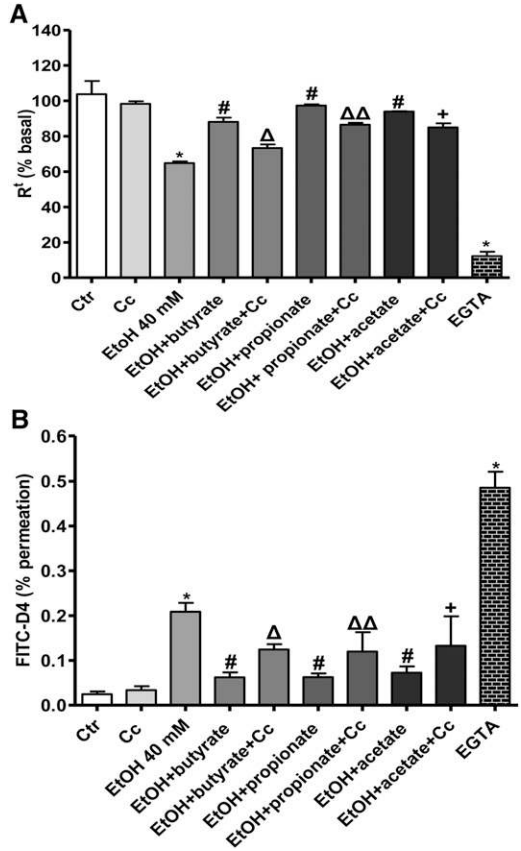

FIGURE 5 Effects of AMPK inhibition by Cc on SCFA–promoted effects on barrier function in Caco-2 monolayers treated with 0.01 mmol/L Cc in the presence or absence of EtOH for 3 h. Effects of butyrate, propionate, or acetate on ethanol-induced decrease in transepithelial electrical resistance (R^t) (*A*) and increase in fluorescein isothiocyanate-labeled dextran 4 kDa (FITC-D4) permeation (*B*) were evaluated. Values are presented as means ± SDs, $n = 6$. *Significantly different from Ctr, $P < 0.05$; #significantly different from ethanol, $P < 0.05$; $^{\Delta,\Delta\Delta,+}$significantly different from ethanol after pretreatment with butyrate, propionate, and acetate, respectively, $P < 0.05$. AMPK, AMP-activated protein kinase; Cc, compound C; Ctr, control; EGTA, ethylene glycol tetraacetic acid; EtOH, ethanol.

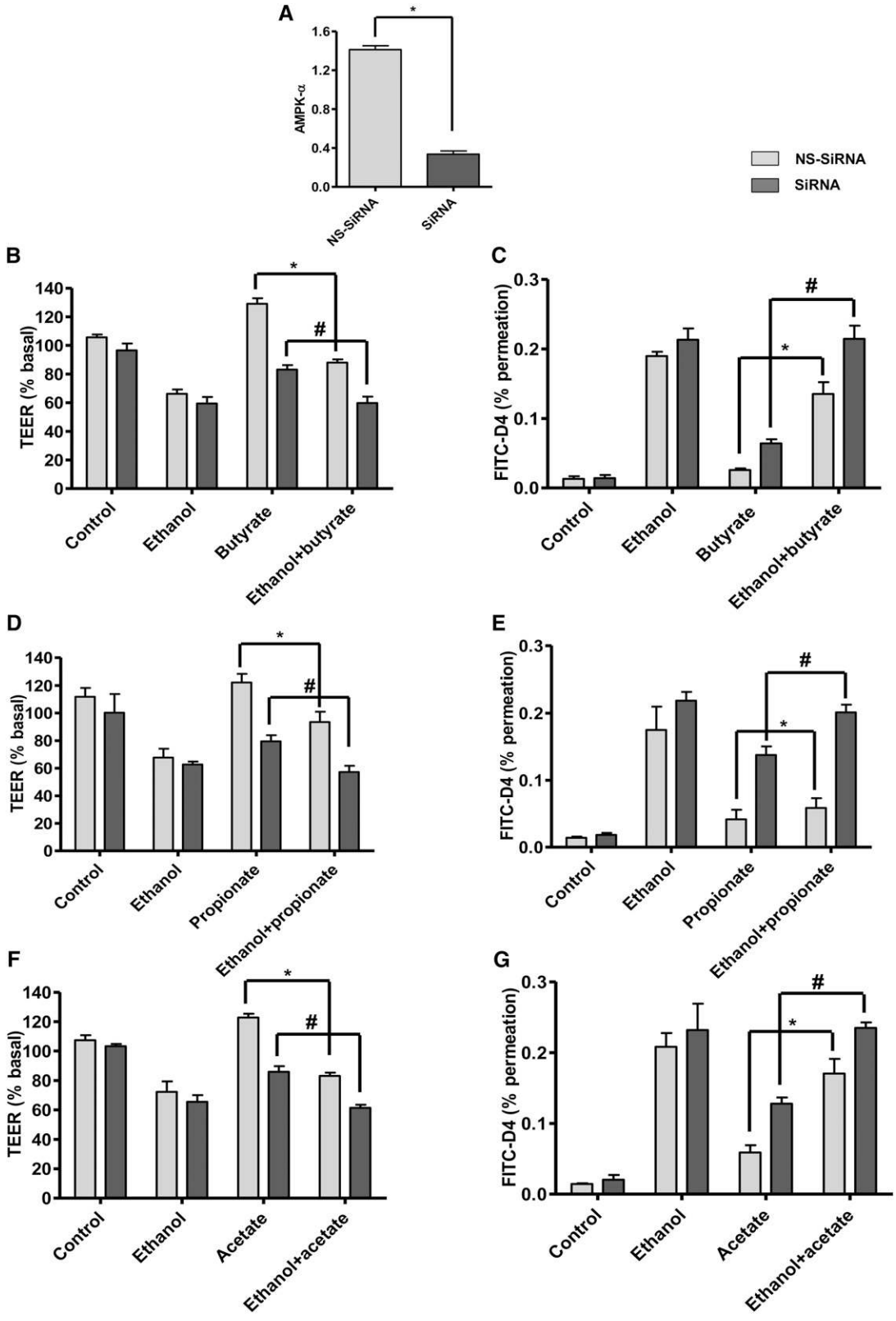

FIGURE 6 Effects of AMPK-α2 knockdown on SCFA–promoted effects on barrier function in ethanol-treated monolayers after transfection of AMPK-α2 with either specific siRNA or NS-RNA. (*A*) AMPK protein levels, values are means ± SDs, $n = 3$. *Significantly different from the value for NS-RNA, $P < 0.01$. Percentage of basal TEER measured after treatment with ethanol in medium with or without pretreatment with butyrate (*B*), propionate (*C*), and acetate (*D*). Values are means ± SDs, $n = 3$. $^{*}P < 0.05$ vs. corresponding ethanol-exposed monolayers; $^{\#}P < 0.01$ vs. corresponding NS-RNA. Percentage of FITC-D4 permeation measured after 3 h of exposure to ethanol in medium with or without pretreatment with butyrate (*E*), propionate (*F*), and acetate (*G*). Values are means ± SDs, $n = 3$. $^{*}P < 0.05$ vs. ethanol-exposed monolayers; $^{\#}P < 0.05$ vs. corresponding NS-RNA. AMPK, AMP-activated protein kinase; FITC-D4, fluorescein isothiocyanate-labeled dextran 4 kDa; NS-RNA, nonspecific RNA; siRNA, small interfering RNA; TEER, transepithelial electrical resistance.

induces an increase in ROS generation, mitochondrial dysfunction, and a decrease in intracellular ATP levels. Our data are in line with numerous studies documenting that ROS and nitrogen oxygen species generation can induce oxidation and nitration of cytoskeletal proteins, respectively, with subsequent increase in intestinal permeability (2,36–38). Although not tested in this study, the potential mechanisms of ethanol-induced ROS generation are most likely to involve a number of ROS-related pathways. Previously, it has been demonstrated that activation of intestinal inducible nitric oxide synthase (2), cytochrome-P450 2E1 (31), and xanthine oxidase (39) mediates ethanol-induced ROS production and, consequently, barrier dysfunction. In the current investigation, we demonstrated that SCFAs protected intestinal monolayers against ethanol and restored normal barrier function. Our data support observations in vitro and in animals that SCFAs can enhance intestinal barrier function (22,24,40). The SCFA concentrations used in the present study were based on those found in the intestinal lumen after dietary fiber supplementation (41) and taking into account the relative molar ratios (14). Furthermore, Suzuki et al. (22) have shown that butyrate, propionate, and acetate at concentrations similar to those we used are able to promote epithelial barrier function in rat large intestine. Interestingly, in our study, treatment with 80 mmol/L acetate (pH 8.47) significantly increased permeability via mechanisms independent of the pH, indicating its potential cytotoxicity. Previously, exposure to acetate > 12.5 mmol/L for 72 h was shown to compromise human gastric epithelial cell viability (42). The discrepancy with our data from 40 mmol/L acetate can be explained by differences in cell type and duration of exposure. Because osmolality can also be involved in the effects of 40 and 80 mmol/L acetate, only the 8 mmol/L concentration was used in additional analyses.

The ethanol-induced abnormal localization of TJs, disorganization, and increase in F-actin protein levels could partially be prevented by SCFAs, suggesting that the facilitating effects of the SCFAs on barrier function may involve reorganization of F-actin and, indirectly, assembly of the TJs. These findings are akin to previous data demonstrating that butyrate can attenuate deoxycholic acid-induced actin cytoskeleton remodeling and actin stress in colonic epithelial cells (43). Furthermore, SCFAs have been reported to enhance the intestinal barrier by stabilizing TJ integrity (24). We speculate that the attenuating effects of SCFAs on ethanol-induced barrier dysfunction in Caco-2 monolayers might be attributable to SCFA-facilitated F-actin ring reorganization and a decrease of stress-fiber formation.

Using concentrations comparable with those used in our study, it has been reported that butyrate (C4:0), propionate (C3:0), and acetate (C2:0) can enhance TEER in Caco-2 monolayers (22, 44). However, the effects propionate and acetate on barrier function were observed with higher concentrations when compared with butyrate, indicating that chain length may determine bioactivity of the SCFAs. Increasing carbon chain length has also been shown to influence the potential effects of SCFAs with regard to, for example, inflammation, carcinogenesis, and barrier function (45). This may partially be related to the ability of SCFAs to cross cell membranes because of the reduced lipid solubility with decreasing chain length (46).

In this study, ethanol induced oxidative stress in Caco-2 cells, and SCFAs were able to inhibit ethanol-induced ROS generation. These findings are in line with previously reported data on the antioxidant potential of SCFAs (17). Increased ROS production and consequently impaired mitochondrial function may cause ATP depletion, a factor that can further contribute to barrier dysfunction (35,47). We also demonstrated that SCFAs can attenuate and prevent ethanol-induced mitochondrial dysfunction and ATP depletion, indicating the potential capacity of SCFAs to protect the intestinal epithelial cells from ethanol-mediated cell metabolic stress. In line with these findings, butyrate has been shown previously to increase ATP stores in Caco-2 cells (48). Particularly intriguing are the recent observations in a rat model of ALD, showing that oats supplementation attenuates ethanol-induced intestinal hyperpermeability and alcoholic steatohepatitis (49) via antioxidant mechanisms. These observations raise the possibility that SCFAs, as produced from fibers as in oats, could protect the intestinal epithelium against ethanol-induced gut leakiness, endotoxemia, and subsequent liver injury in humans.

Because SCFAs constitute a major energy source in the colon and ethanol can interfere with ATP production (50), the role of AMPK activation in effects of SCFAs on ethanol-induced barrier dysfunction has been explored. This serine/threonine protein kinase is activated during cellular stress, resulting in elevation of intracellular ATP (51). In addition, AMPK has been shown to modulate the TJ integrity in Madin-Darby canine kidney cell monolayers (52,53). Our data revealed that the SCFAs can induce AMPK activation (phosphorylation) in a magnitude comparable with the effects of AICAR, which has been found previously to promote epithelial barrier function through AMPK activation (52). Pretreatment with Cc inhibited the SCFA-induced AMPK activation and abolished the ability of the SCFAs to improve the barrier function, indicating involvement of AMPK. Furthermore, using siRNA targeting AMPK under the same conditions supported the role of AMPK as a regulatory protein of intestinal barrier protection by SCFAs. Our data confirm previous reports demonstrating that AMPK activity is required for butyrate-facilitated TJ assembly (24) and provides new evidence that AMPK activation is also required for the promoting effects of propionate and acetate on barrier function. Because the inhibitory effect of knockdown of AMPK on barrier function was partial, alternative mechanisms underlying the SCFA promotive effects have to be considered.

The Caco-2 cell monolayer model is widely used to assess effects of ethanol and its metabolites, such as acetaldehyde, on intestinal permeability (2,3,32,54–56), but it has some limitations. For instance, other cells involved in intestinal epithelium homeostasis, including goblet and immune cells, were not taken into account. Therefore, additional in vitro experiments using coculture models and in vivo interventional studies with, for example, fermentable fibers, should evaluate the effects of SCFAs, separately or in combination, on ethanol as well as its other metabolites, including acetaldehyde, on intestinal epithelial barrier function. In addition, using intestinal cells in a coculture model will be a useful tool to examine effects of SCFAs on acetaldehyde-induced carcinogenesis.

In summary, the present study provides evidence that SCFAs can attenuate ethanol-induced intestinal barrier dysfunction and metabolic stress with possible underlying mechanisms, including facilitation of the TJ assembly and F-actin cortical ring rearrangement. Furthermore, the positive effects of SCFAs on barrier function seem to involve, at least in part, AMPK activation. Because increased intestinal permeability can be associated with inflammatory bowel disease and ALD, elucidation of the exact mechanisms underlying these beneficial effects may form a basis for the design of therapeutic or preventive in vivo strategies, enabling SCFAs as potential nutrients to treat and/or prevent ethanol-induced intestinal barrier dysfunction.

Acknowledgments

E.E.E. conducted the experiments, analyzed the data, and wrote the manuscript; D.M.J. and J.D. contributed to the study design; H.-J.P. helped with conducting the experiments; D.M.J. and A.A.M. supervised conduction of the research and revised the manuscript; and A.A.M. had primary responsibility for the final content. All authors read and approved the final manuscript.

Literature Cited

1. Bujanda L. The effects of alcohol consumption upon the gastrointestinal tract. Am J Gastroenterol. 2000;95:3374–82.
2. Banan A, Choudhary S, Zhang Y, Fields JZ, Keshavarzian A. Ethanol-induced barrier dysfunction and its prevention by growth factors in human intestinal monolayers: evidence for oxidative and cytoskeletal mechanisms. J Pharmacol Exp Ther. 1999;291:1075–85.
3. Elamin E, Jonkers D, Juuti-Uusitalo K, van Ijzendoorn S, Troost F, Duimel H, Broers J, Verheyen F, Dekker J, Masclee A. Effects of ethanol and acetaldehyde on tight junction integrity: in vitro study in a three dimensional intestinal epithelial cell culture model. PLoS One. 2012;7: e35008.
4. Keshavarzian A, Fields JZ, Vaeth J, Holmes EW. The differing effects of acute and chronic alcohol on gastric and intestinal permeability. Am J Gastroenterol. 1994;89:2205–11.
5. Bjarnason I, Peters TJ, Wise RJ. The leaky gut of alcoholism: possible route of entry for toxic compounds. Lancet. 1984;1:179–82.
6. Parlesak A, Schafer C, Schutz T, Bode JC, Bode C. Increased intestinal permeability to macromolecules and endotoxemia in patients with chronic alcohol abuse in different stages of alcohol-induced liver disease. J Hepatol. 2000;32:742–7.
7. Bode C, Kugler V, Bode JC. Endotoxemia in patients with alcoholic and non-alcoholic cirrhosis and in subjects with no evidence of chronic liver disease following acute alcohol excess. J Hepatol. 1987;4:8–14.
8. Keshavarzian A, Holmes EW, Patel M, Iber F, Fields JZ, Pethkar S. Leaky gut in alcoholic cirrhosis: a possible mechanism for alcohol-induced liver damage. Am J Gastroenterol. 1999;94:200–7.
9. Rao RK, Seth A, Sheth P. Recent advances in alcoholic liver disease I. Role of intestinal permeability and endotoxemia in alcoholic liver disease. Am J Physiol Gastrointest Liver Physiol. 2004;286:G881–4.
10. Pöschl G, Seitz HK. Alcohol and cancer. Alcohol Alcohol. 2004;39: 155–65.
11. Hamer HM, Jonkers D, Venema K, Vanhoutvin S, Troost FJ, Brummer RJ. Review article: the role of butyrate on colonic function. Aliment Pharmacol Ther. 2008;27:104–19.
12. Cook SI, Sellin JH. Review article: short chain fatty acids in health and disease. Aliment Pharmacol Ther. 1998;12:499–507.
13. Hill MJ. Bacterial fermentation of complex carbohydrate in the human colon. Eur J Cancer Prev. 1995;4:353–8.
14. D'Argenio G, Mazzacca G. Short-chain fatty acid in the human colon. Relation to inflammatory bowel diseases and colon cancer. Adv Exp Med Biol. 1999;472:149–58.
15. Meijer K, de Vos P, Priebe MG. Butyrate and other short-chain fatty acids as modulators of immunity: what relevance for health? Curr Opin Clin Nutr Metab Care. 2010;13:715–21.
16. Huang N, Wu GD. Short chain fatty acids inhibit the expression of the neutrophil chemoattractant, interleukin 8, in the Caco-2 intestinal cell line. Adv Exp Med Biol. 1997;427:145–53.
17. Hamer HM, Jonkers DM, Bast A, Vanhoutvin SA, Fischer MA, Kodde A, Troost FJ, Venema K, Brummer RJ. Butyrate modulates oxidative stress in the colonic mucosa of healthy humans. Clin Nutr. 2009;28:88–93.
18. Hijova E, Chmelarova A. Short chain fatty acids and colonic health. Bratisl Lek Listy. 2007;108:354–8.
19. Clausen MR, Bonnen H, Mortensen PB. Colonic fermentation of dietary fibre to short chain fatty acids in patients with adenomatous polyps and colonic cancer. Gut. 1991;32:923–8.
20. Van Deun K, Pasmans F, Van Immerseel F, Ducatelle R, Haesebrouck F. Butyrate protects Caco-2 cells from Campylobacter jejuni invasion and translocation. Br J Nutr. 2008;100:480–4.
21. Peng L, He Z, Chen W, Holzman IR, Lin J. Effects of butyrate on intestinal barrier function in a Caco-2 cell monolayer model of intestinal barrier. Pediatr Res. 2007;61:37–41.
22. Suzuki T, Yoshida S, Hara H. Physiological concentrations of short-chain fatty acids immediately suppress colonic epithelial permeability. Br J Nutr. 2008;100:297–305.
23. Mariadason JM, Catto-Smith A, Gibson PR. Modulation of distal colonic epithelial barrier function by dietary fibre in normal rats. Gut. 1999;44:394–9.
24. Peng L, Li ZR, Green RS, Holzman IR, Lin J. Butyrate enhances the intestinal barrier by facilitating tight junction assembly via activation of AMP-activated protein kinase in Caco-2 cell monolayers. J Nutr. 2009; 139:1619–25.
25. Corton JM, Gillespie JG, Hardie DG. Role of the AMP-activated protein kinase in the cellular stress response. Curr Biol. 1994;4:315–24.
26. Manzo-Avalos S, Saavedra-Molina A. Cellular and mitochondrial effects of alcohol consumption. Int J Environ Res Public Health. 2010;7: 4281–304.
27. Corton JM, Gillespie JG, Hawley SA, Hardie DG. 5-aminoimidazole-4-carboxamide ribonucleoside. A specific method for activating AMP-activated protein kinase in intact cells? Eur J Biochem. 1995; 229:558–65.
28. Tao N, Sussman S, Nieto J, Tsukamoto H, Yuan JM. Demographic characteristics of hospitalized patients with alcoholic liver disease and pancreatitis in Los Angeles county. Alcohol Clin Exp Res. 2003;27: 1798–804.
29. Uc A, Stokes JB, Britigan BE. Heme transport exhibits polarity in Caco-2 cells: evidence for an active and membrane protein-mediated process. Am J Physiol Gastrointest Liver Physiol. 2004;287:G1150–7.
30. Swanson G, Forsyth CB, Tang Y, Shaikh M, Zhang L, Turek FW, Keshavarzian A. Role of intestinal circadian genes in alcohol-induced gut leakiness. Alcohol Clin Exp Res. 2011;35:1305–14.
31. McCarroll JA, Phillips PA, Park S, Doherty E, Pirola RC, Wilson JS, Apte MV. Pancreatic stellate cell activation by ethanol and acetaldehyde: is it mediated by the mitogen-activated protein kinase signaling pathway? Pancreas. 2003;27:150–60.
32. Forsyth CB, Tang Y, Shaikh M, Zhang L, Keshavarzian A. Alcohol stimulates activation of Snail, epidermal growth factor receptor signaling, and biomarkers of epithelial-mesenchymal transition in colon and breast cancer cells. Alcohol Clin Exp Res. 2010;34:19–31.
33. Banan A, Smith GS, Rieckenberg CL, Kokoska ER, Miller TA. Protection against ethanol injury by prostaglandin in a human intestinal cell line: role of microtubules. Am J Physiol. 1998;274:G111–21.
34. Zhong W, Zhao Y, McClain CJ, Kang YJ, Zhou Z. Inactivation of hepatocyte nuclear factor-4{alpha} mediates alcohol-induced down-regulation of intestinal tight junction proteins. Am J Physiol Gastrointest Liver Physiol. 2010;299:G643–51.
35. Lewis K, McKay DM. Metabolic stress evokes decreases in epithelial barrier function. Ann N Y Acad Sci. 2009;1165:327–37.
36. Forsyth CB, Farhadi A, Jakate SM, Tang Y, Shaikh M, Keshavarzian A. Lactobacillus GG treatment ameliorates alcohol-induced intestinal oxidative stress, gut leakiness, and liver injury in a rat model of alcoholic steatohepatitis. Alcohol. 2009;43:163–72.
37. Keshavarzian A, Farhadi A, Forsyth CB, Rangan J, Jakate S, Shaikh M, Banan A, Fields JZ. Evidence that chronic alcohol exposure promotes intestinal oxidative stress, intestinal hyperpermeability and endotoxemia prior to development of alcoholic steatohepatitis in rats. J Hepatol. 2009;50:538–47.
38. Zhong W, McClain CJ, Cave M, Kang YJ, Zhou Z. The role of zinc deficiency in alcohol-induced intestinal barrier dysfunction. Am J Physiol Gastrointest Liver Physiol. 2010;298:G625–33.
39. Lieber CS. Ethanol metabolism, cirrhosis and alcoholism. Clin Chim Acta. 1997;257:59–84.
40. Wang HB, Wang PY, Wang X, Wan YL, Liu YC. Butyrate enhances intestinal epithelial barrier function via up-regulation of tight junction protein Claudin-1 transcription. Dig Dis Sci. 2012;57:3126–35.
41. Topping DL, Clifton PM. Short-chain fatty acids and human colonic function: roles of resistant starch and nonstarch polysaccharides. Physiol Rev. 2001;81:1031–64.
42. Sun J, Bi L, Chi Y, Aoki K, Misumi J. Effect of sodium acetate on cell proliferation and induction of proinflammatory cytokines: a preliminary evaluation. Food Chem Toxicol. 2005;43:1773–80.
43. Looby E, Long A, Kelleher D, Volkov Y. Bile acid deoxycholate induces differential subcellular localisation of the PKC isoenzymes beta 1, epsilon and delta in colonic epithelial cells in a sodium butyrate insensitive manner. Int J Cancer. 2005;114:887–95.

44. Mariadason JM, Barkla DH, Gibson PR. Effect of short-chain fatty acids on paracellular permeability in Caco-2 intestinal epithelium model. Am J Physiol. 1997;272:G705–12.
45. Morgan TR, Mandayam S, Jamal MM. Alcohol and hepatocellular carcinoma. Gastroenterology. 2004;127:S87–96.
46. DeSoignie R, Sellin JH. Propionate-initiated changes in intracellular pH in rabbit colonocytes. Gastroenterology. 1994;107:347–56.
47. Unno N, Menconi MJ, Salzman AL, Smith M, Hagen S, Ge Y, Ezzell RM, Fink MP. Hyperpermeability and ATP depletion induced by chronic hypoxia or glycolytic inhibition in Caco-2BBe monolayers. Am J Physiol. 1996;270:G1010–21.
48. Wang A, Si H, Liu D, Jiang H. Butyrate activates the cAMP-protein kinase A-cAMP response element-binding protein signaling pathway in Caco-2 cells. J Nutr. 2012;142:1–6.
49. Tang Y, Forsyth CB, Banan A, Fields JZ, Keshavarzian A. Oats supplementation prevents alcohol-induced gut leakiness in rats by preventing alcohol-induced oxidative tissue damage. J Pharmacol Exp Ther. 2009;329:952–8.
50. Cunningham CC, Van Horn CG. Energy availability and alcohol-related liver pathology. Alcohol Res Health. 2003;27:291–9.
51. Hardie DG. The AMP-activated protein kinase pathway–new players upstream and downstream. J Cell Sci. 2004;117:5479–87.
52. Zhang L, Li J, Young LH, Caplan MJ. AMP-activated protein kinase regulates the assembly of epithelial tight junctions. Proc Natl Acad Sci USA. 2006;103:17272–7.
53. Zheng B, Cantley LC. Regulation of epithelial tight junction assembly and disassembly by AMP-activated protein kinase. Proc Natl Acad Sci USA. 2007;104:819–22.
54. Asai K, Buurman WA, Reutelingsperger CP, Schutte B, Kaminishi M. Modular effects of estradiol on ethanol-induced apoptosis in human intestinal epithelial cells. Scand J Gastroenterol. 2005;40:326–35.
55. Ma TY, Nguyen D, Bui V, Nguyen H, Hoa N. Ethanol modulation of intestinal epithelial tight junction barrier. Am J Physiol. 1999;276:G965–74.
56. Rao RK. Acetaldehyde-induced barrier disruption and paracellular permeability in Caco-2 cell monolayer. Methods Mol Biol. 2008;447:171–83.